

# Compton reflection in AGN with *Simbol-X*

V. Beckmann\*, T.J.-L. Courvoisier\*, N. Gehrels<sup>†</sup>, P. Lubiński\*\*, J. Malzac<sup>‡</sup>,  
P. O. Petrucci<sup>§</sup>, C. R. Shrader<sup>†</sup> and S. Soldi\*

\**ISDC Data Centre for Astrophysics, Ch. d'Ecogia 16, 1290 Versoix, Switzerland*

<sup>†</sup>*NASA Goddard Space Flight Center, Code 661, Greenbelt, MD 20771, USA*

\*\**Centrum Astronomiczne im. M. Kopernika, Bartycka 18, PL-00-716 Warszawa, Poland*

<sup>‡</sup>*CESR, OMP, UPS, CNRS; B.P. 44346, 31028 Toulouse Cedex 4, France*

<sup>§</sup>*Laboratoire d'Astrophysique de Grenoble, CNRS, UMR 5571, BP 53X, 38041 Grenoble, France*

**Abstract.** AGN exhibit complex hard X-ray spectra. Our current understanding is that the emission is dominated by inverse Compton processes which take place in the corona above the accretion disk, and that absorption and reflection in a distant absorber play a major role. These processes can be directly observed through the shape of the continuum, the Compton reflection hump around 30 keV, and the iron fluorescence line at 6.4 keV. We demonstrate the capabilities of *Simbol-X* to constrain complex models for cases like MCG-05-23-016, NGC 4151, NGC 2110, and NGC 4051 in short (10 ksec) observations. We compare the simulations with recent observations on these sources by INTEGRAL, Swift and Suzaku. Constraining reflection models for AGN with *Simbol-X* will help us to get a clear view of the processes and geometry near to the central engine in AGN, and will give insight to which sources are responsible for the Cosmic X-ray background at energies  $> 20$  keV.

**Keywords:** Galaxies: active – Galaxies: Seyfert – X-rays: galaxies

**PACS:** 95.55.Ka, 98.54.Cm

## WHY IS COMPTON-REFLECTION IN AGN OF IMPORTANCE?

The extragalactic X-ray sky is dominated by active galactic nuclei (AGN) and clusters of galaxies. Studying the population of sources in X-ray bands has been a challenge ever since the first observations by rocket borne X-ray detectors. Above 2 keV a synopsis of previous results is as follows: the 2 – 10 keV Seyfert 1 continua are approximated by a  $\Gamma \simeq 1.9$  powerlaw form [17]. A flattening above  $\sim 10$  keV has been noted, and is commonly attributed to Compton reflection [5]. There is a great deal of additional detail in this spectral domain: “warm” absorption, multiple-velocity component outflows, and relativistic line broadening. The Seyfert 2 objects are more poorly categorized here, but the general belief is that they are intrinsically equivalent to the Seyfert 1s, but viewed through much larger absorption columns.

Above 20 keV the empirical picture is less clear. The  $\sim 20 - 200$  keV continuum shape of both Seyfert types is consistent with a thermal Comptonization spectral form, although in all but a few cases the data are not sufficiently constraining to rule out a pure powerlaw form with photon index  $\Gamma \simeq 2.0$  for Seyfert 1 and  $\Gamma \simeq 1.8$  for Seyfert 2 [4]. Nonetheless, the non-thermal scenarios with pure powerlaw continua extending to  $\sim$  MeV energies reported in the pre-*CGRO* era are no longer widely believed, and are likely a result of background systematics. However, a detailed picture of the Comptonizing plasma - its spatial, dynamical, and thermo-dynamical structure - is not known. Among the critical determinations which *Simbol-X* can provide are the plasma temperature and

optical depth (or Compton “Y” parameter) for a large sample of objects. In order to understand the physical processes and the location of the processing regions with respect to the central black hole in AGN, a decoupling of the components is essential. *Simbol-X* will help to determine exact measurements of the Compton reflection strength together with the continuum shape and the strength and width of the iron  $K\alpha$  fluorescence line.

Related to the compilation of AGN surveys in the hard X-rays is the question of what sources form the cosmic X-ray background (CXB). The most reliable measurement in the 10 - 500 keV has been provided by *HEAO 1 A-4*, showing that the CXB peaks at an energy of about 30keV [6]. The isotropic nature of the X-ray background points to an extragalactic origin, and as the brightest persistent sources are AGNs, it was suggested early on that those objects are the main source of the CXB [12]. In the soft X-rays this concept has been proven to be correct through the observations of the *ROSAT* deep X-ray surveys, which showed that 90% of the 0.5 – 2.0keV CXB can be resolved into AGNs [10]. At higher energies (2 – 10keV), *ASCA* and *Chandra* surveys measured the hard X-ray luminosity function (XLF) of AGNs and its cosmological evolution. These studies show that in this energy range the CXB can be explained by AGNs, but with a higher fraction of absorbed ( $N_H > 10^{22} \text{ cm}^{-2}$ ) objects than in the soft X-rays (e.g. [15]). A study based on the *RXTE* survey by Sazonov & Revnivtsev [9] derived the local hard X-ray luminosity function of AGNs in the 3–20 keV band. They showed that the summed emissivity of AGNs in this energy range is smaller than the total X-ray volume emissivity in the local Universe, and suggested that a comparable X-ray flux may be produced together by lower luminosity AGNs, non-active galaxies and clusters of galaxies. Using the *HEAO 1-A2* AGNs, Shinozaki et al. (2006), however, obtained a local AGN emissivity which is about twice larger than the value of Sazonov & Revnivtsev [9].

*INTEGRAL* and *Swift* added substantial information to the nature of bright AGNs in the hard X-rays in the local Universe. Considering the expected composition of the hard X-ray background, it does not currently appear that the population detected by these missions can explain the peak at 30 keV, as Compton thick AGNs are apparently less abundant than expected [2, 14]. The fraction of Compton thick AGNs is found to be small (< 5%, [4]). Evolution of the source population can play a major role in the sense that the fraction of absorbed sources among AGNs might be correlated with redshift [16]. *INTEGRAL* and *Swift* probe the AGN population in the local Universe ( $z < 0.1$ ). Because of this *INTEGRAL/IBIS* and *Swift/BAT* surveys will most likely not be able to test evolutionary scenarios of AGNs and thus will be inadequate to explain the cosmic X-ray background at  $E > 20\text{keV}$ . Future missions with focusing optics such as *Simbol-X* are required to answer the question of what dominates the Universe in the hard X-rays.

## MEASUREMENTS COMPARED TO SIMBOL-X SIMULATIONS

The strength of the Compton reflection component has been measured using hard X-ray data from various missions, such as *BeppoSAX*, *INTEGRAL*, *Suzaku*, often in combination with soft X-ray measurements from *XMM-Newton*, *Chandra*, and *Swift/XRT*. The reflection strength  $R$  is defined as the relative amount of reflection compared to the directly viewed primary spectrum. For some objects relative reflection values of  $R > 1$

**TABLE 1.** Reflection measurements for 4 different Seyfert galaxies, based on *INTEGRAL* and other missions, compared with *Simbol-X* simulations

	NGC 4151	NGC 2110	MCG-5-23-16	NGC 4051
$f_{20-40\text{keV}}$ [erg cm <sup>-2</sup> s <sup>-1</sup> ]	$24 \times 10^{-11}$	$7.4 \times 10^{-11}$	$6 \times 10^{-11}$	$2 \times 10^{-11}$
<i>INTEGRAL</i> exposure	400 ks	160 ks	310 ks	700 ks
reflection ( <i>INTEGRAL</i> )	$R = 1.0^{+0.4}_{-0.3}$ [1]	$R < 0.1$	$R < 0.25$ [3]	$R = 5.6$
Other observatory	<i>BeppoSAX</i> + <i>XMM</i>	<i>BeppoSAX</i>	<i>Suzaku</i> [7]	<i>Suzaku</i>
reflection	$R \sim 2$ [11]	$R < 0.4$ [8]	$R = 1.1 \pm 0.2$	$R \sim 7$ [13]
Simbol-X simulation input	$R = 1.0$	$R = 0$	$R = 0$	$R = 0.5$
Simbol-X output	$R = 1.0 \pm 0.1$	$R < 0.04$	$R < 0.1$	$R = 0.6 \pm 0.2$

have been reported. This implies that more primary X-ray radiation is emitted toward the reflector than toward the observer due to e.g. relativistic effects caused by a dynamic corona moving towards the reflecting disk or light bending effects, or a special geometry with a high intrinsic covering fraction of the cold disk material. This can also be explained by variable emission of the central engine and a time delay between the underlying continuum and the reflected component from remote material. In the following and in Tab. 1, we compare the measured reflection strength with what can be expected in 10 ksec observations by *Simbol-X*:

**NGC 4151** This source is among the brightest AGN in the hard X-ray sky. Based on a 400 ks observation, *INTEGRAL* data allowed to constrain the reflection strength to  $R = 1.0^{+0.4}_{-0.3}$  [1], consistent with an earlier measurement based on *XMM-Newton* and *BeppoSAX* data ( $R \sim 2$ , [11]). A 10 ks *Simbol-X* observation would allow to constrain the value to 10%.

**NGC 2110** *BeppoSAX* observations constrained the reflection component to  $R < 0.4$  [8], and recent simultaneous *INTEGRAL*/IBIS and *Swift*/XRT data resulted in  $R < 0.1$ . A *Simbol-X* simulation, assuming  $R = 0$  resulted in an upper limit of  $R < 0.04$ .

**MCG-5-23-16** *INTEGRAL* combined with simultaneous *Swift*/XRT data gave an upper limit of  $R < 0.25$  [3], while a 220 ks *Suzaku* observation derived  $R = 1.1 \pm 0.2$  [7], leading to the conclusion that the reflection component is variable in this source. If indeed  $R = 0$ , *Simbol-X* will be able to constrain this value to  $R < 0.1$  within 10 ks.

**NGC 4051** This source exhibits the strongest reflection component measured so far, with  $R = 5.6$  (700 ks *INTEGRAL*) and  $R \simeq 7$  (80 ks *Suzaku*, [13]). A source at the flux level of NGC 4051 but with a reflection component  $R = 0.5$  can be constrained to  $R = 0.6 \pm 0.2$  in a 10 ks *Simbol-X* observation (Fig. 1).

## CONCLUSIONS

While the reflection strength is already rather well constrained in a few X-ray bright AGN with  $f_{20-40\text{keV}} > 5 \times 10^{-11}$  erg cm<sup>-2</sup> s<sup>-1</sup> by data from existing missions, focusing optics as provided by *Simbol-X* are necessary in order to significantly increase our knowledge about how frequent strong reflection components are in AGN in general. In order to answer the question, whether the known AGN population in the local universe is

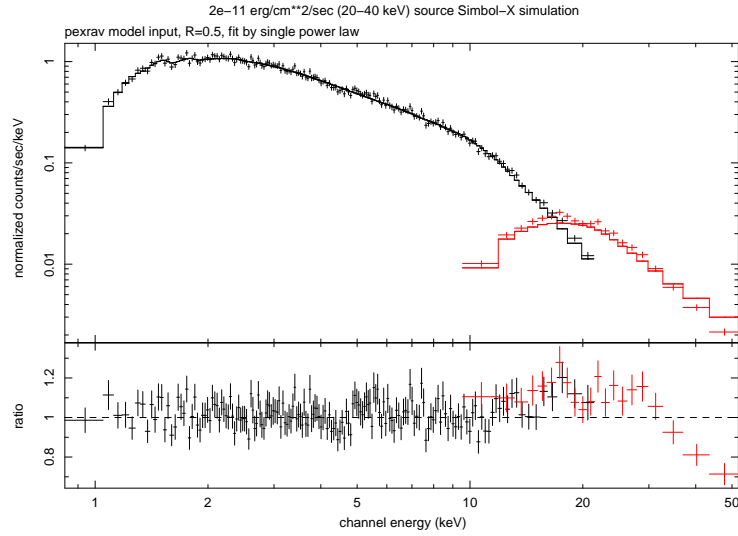


**FIGURE 1.** Simbol-X simulation. The simulated spectrum with a reflection strength of  $R = 0.5$  is fitted by a single power law model. The residuals above 15 keV show the effect of the missing reflection component in the model.

sufficient to explain the CXB, or whether evolution has to be taken into account, *Simbol-X* will reveal whether in the majority of AGN  $R \simeq 0$ ,  $R \simeq 1$ , or  $R \gg 1$ . This will also answer the question, how important reflection really is in the view of the central engine. 10 ks observations are sufficient to constrain  $R$  to 10 – 20% at the  $2 \times 10^{-11} \text{ erg cm}^{-2} \text{ s}^{-1}$  flux level. The second *INTEGRAL* AGN catalogue [4] includes 55 AGN above this flux level. These simulations show also that with *Simbol-X* the study of the reflection component simultaneously with the iron line will be possible for the first time on a dynamical time scale. This will provide crucial information for our understanding of the reflection component itself and of the AGN environment in general.

## REFERENCES

1. V. Beckmann, C. R. Shrader, N. Gehrels, et al., *ApJ* **634**, 939 (2005)
2. V. Beckmann, S. Soldi, C. R. Shrader, N. Gehrels, N. Produit, *ApJ* **652**, 126 (2006)
3. V. Beckmann, T.J.-L. Courvoisier, N. Gehrels, et al., *A&A* **492**, 93 (2008)
4. V. Beckmann, S. Soldi, C. Ricci et al., *A&A* submitted (2009)
5. I. M. George, and A. C. Fabian, *MNRAS* **249**, 352 (1991)
6. D. E. Gruber, J. L. Matteson, L. E. Peterson, G. V. Jung, *ApJ* **520**, 124 (1999)
7. J. N. Reeves, H. Awaki, G. C. Dewangan et al., *PASJ* **59**, 301 (2007)
8. G. Risaliti, *A&A* **386**, 379 (2002)
9. S. Y. Sazonov, and M. G. Revnivtsev, *A&A* **423**, 469 (2004)
10. M. Schmidt et al., *A&A* **329**, 495 (1998)
11. N. J. Schurch, R. S. Warwick, R. E. Griffiths, S. Sembay, *MNRAS* **345**, 423 (2003)
12. G. Setti, L. Woltjer, *A&A*, **224**, L21 (1989)
13. Y. Terashima, L. C. Gallo, H. Inoue, et al., *PASJ* accepted, arXiv:0811.0692 (2009)
14. E. Treister, and C. M. Urry, *ApJ* **630**, 115 (2005)
15. Y. Ueda, M. Akiyama, K. Ohta, T. Miyaji, *ApJ* **598**, 886 (2003)
16. M. A. Worsley et al., *MNRAS* **357**, 1281 (2005)
17. A. A. Zdziarski, W. N. Johnson, C. Done, D. Smith, K. McNaron-Brown, *ApJ* **438**, L63 (1995)